Title

The Novel bis-1,2,4-Triazine MIPS-0004373 Demonstrates Rapid and Potent Activity against All Blood Stages of the Malaria Parasite.

Journal

Antimicrobial Agents and Chemotherapy, 65(11)

Authors

Ellis, Katherine

Lucantoni, Leonardo

Chavchich, Marina

et al.

Publication Date

2021-10-18

DOI

10.1128/AAC.00311-21

Peer reviewed

AMERICAN SOCIETY FOR MICROBIOLOGY | Antimicrobial Agents and Chemotherapy®

MECHANISMS OF ACTION: PHYSIOLOGICAL EFFECTS

The Novel bis-1,2,4-Triazine MIPS-0004373 Demonstrates Rapid and Potent Activity against All Blood Stages of the Malaria Parasite

Katherine M. Ellis,[a] Leonardo Lucantoni,[b] Marina Chavchich,[c] Matthew Abraham,[d] Amanda De Paoli,[a] Madeline R. Luth,[d] Anne-Marie Zeeman,[e] Michael J. Delves,[f*] Fernando Sánchez-Román Terán,[f§] Ursula Straschil,[f] Jake Baum,[f] Clemens H. M. Kocken,[e] Stuart A. Ralph,[g] Elizabeth A. Winzeler,[d] Vicky M. Avery,[b] Michael D. Edstein,[c] Jonathan B. Baell,[h] Darren J. Creek[a]

[a]Drug Delivery Disposition and Dynamics, Monash Institute of Pharmaceutical Sciences, Monash University, Parkville, VIC, Australia
[b]Discovery Biology, Griffith University, Nathan, QLD, Australia
[c]The Department of Drug Evaluation, Australian Defence Force Malaria and Infectious Disease Institute, Brisbane, QLD, Australia
[d]School of Medicine, University of California, San Diego, La Jolla, California, USA
[e]Department of Parasitology, Biomedical Primate Research Centre, Rijswijk, Netherlands
[f]Department of Life Sciences, Imperial College London, South Kensington, London, United Kingdom
[g]Department of Biochemistry and Molecular Biology, Bio21 Molecular Science and Biotechnology Institute, The University of Melbourne, Parkville, VIC, Australia
[h]Medicinal Chemistry, Monash Institute of Pharmaceutical Sciences, Monash University, Parkville, VIC, Australia

ABSTRACT Novel bis-1,2,4-triazine compounds with potent *in vitro* activity against *Plasmodium falciparum* parasites were recently identified. The bis-1,2,4-triazines represent a unique antimalarial pharmacophore and are proposed to act by a novel but as-yet-unknown mechanism of action. This study investigated the activity of the bis-1,2,4-triazine MIPS-0004373 across the mammalian life cycle stages of the parasite and profiled the kinetics of activity against blood and transmission stage parasites *in vitro* and *in vivo*. MIPS-0004373 demonstrated rapid and potent activity against *P. falciparum*, with excellent *in vitro* activity against all asexual blood stages. Prolonged *in vitro* drug exposure failed to generate stable resistance *de novo*, suggesting a low propensity for the emergence of resistance. Excellent activity was observed against sexually committed ring stage parasites, but activity against mature gametocytes was limited to inhibiting male gametogenesis. Assessment of liver stage activity demonstrated good activity in an *in vitro P. berghei* model but no activity against *Plasmodium cynomolgi* hypnozoites or liver schizonts. The bis-1,2,4-triazine MIPS-0004373 efficiently cleared an established *P. berghei* infection *in vivo*, with efficacy similar to that of artesunate and chloroquine and a recrudescence profile comparable to that of chloroquine. This study demonstrates the suitability of bis-1,2,4-triazines for further development toward a novel treatment for acute malaria.

KEYWORDS malaria, antimalarial, triazine, *Plasmodium*

Malaria is a parasitic disease caused by infection of red blood cells with the *Plasmodium* parasite. More than 40% of the world's population live in areas where malaria is endemic, and each year there are over 200 million reported cases of malaria. Over 400,000 of these cases result in death, placing malaria as one of the most significant human parasitic diseases (1). Artemisinin-based combination therapies (ACTs) are currently the first-line treatments for malaria. While these drug combinations initially displayed a high level of efficacy (2), there have been increasing reports of ACT resistance in Southeast Asia over the last decade (3). Since very few novel antimalarial compounds have reached clinical approval in recent times, the increase in parasite resistance to current first-line treatments highlights an urgent need for the discovery of new antimalarial medicines (4).

Citation Ellis KM, Lucantoni L, Chavchich M, Abraham M, De Paoli A, Luth MR, Zeeman A-M, Delves MJ, Terán FS-R, Straschil U, Baum J, Kocken CHM, Ralph SA, Winzeler EA, Avery VM, Edstein MD, Baell JB, Creek DJ. 2021. The novel bis-1,2,4-triazine MIPS-0004373 demonstrates rapid and potent activity against all blood stages of the malaria parasite. Antimicrob Agents Chemother 65:e00311-21. https://doi.org/10.1128/AAC.00311-21.

Address correspondence to Jonathan B. Baell, jonathan.baell@monash.edu, or Darren J. Creek, darren.creek@monash.edu.

* Present address: Michael J. Delves, London School of Hygiene and Tropical Medicine, London, United Kingdom

§Present address: Fernando Sánchez-Román Terán, Kings College London, London, United Kingdom.

Received 16 February 2021
Returned for modification 28 April 2021
Accepted 11 August 2021
Accepted manuscript posted online 30 August 2021
Published 18 October 2021

TABLE 1 Summary of MMV target candidate profiles (TCPs) for new antimalarial medicines (4)

Profile	Intended use
TCP-1	Molecules that clear asexual blood stage parasitemia
TCP-3	Molecules with activity against hypnozoites (mainly *P. vivax*)
TCP-4	Molecules with activity against hepatic schizonts
TCP-5	Molecules that block transmission (targeting parasite gametocytes)
TCP-6	Molecules that block transmission by targeting the insect vector (endectocides)

The successful development of a new antimalarial will require the drug to demonstrate excellent efficacy, minimal toxicity, low cost, and a lack of cross-resistance to existing drugs (5). Furthermore, a recent shift in focus from malaria control to total eradication highlights the necessity for alternative antimalarials with specific activity profiles. New drugs for the treatment of clinical symptoms of blood stage malaria infection, relapsing malaria, and severe malaria or for mass drug administration for treatment and transmission blocking are required. Strategies for chemoprevention in areas of endemicity or chemoprotection for migratory populations as well as outbreak prevention are required. To facilitate the efficient development of drug candidates, the Medicines for Malaria Venture (MMV) have outlined desired target candidate profiles (TCPs) for new antimalarials (Table 1) (4).

These target candidate profiles provide guidance regarding the assessment of drug efficacy, pharmacokinetics, and toxicity before a compound is progressed toward clinical trials. Ideal requirements of novel antimalarials include potent and rapid clearance of blood stage parasites, suitability as a component of a combination therapy, pharmacokinetics that provide therapeutic blood concentrations for an extended period after a single oral dose, a low toxicity profile, absence of detrimental drug-drug interactions with relapse prevention or transmission blocking molecules, and minimal risk of developing resistance. In addition, activity against other stages of the parasite life cycle would be an attractive feature to provide the opportunity for prophylactic or transmission-blocking activity.

The bis-1,2,4-triazines represent a new class of antimalarial compounds with potent activity against *P. falciparum* that were identified by screening chemical libraries (6). These compounds, based on a bis-1,2,4-triazine dimer core structure, are currently undergoing optimization by iterative rounds of medicinal chemistry and *in vitro* testing in order to improve potency, selectivity, and metabolic stability. A lead triazine dimer, MIPS-0004373 (Fig. 1), was shown to be highly active *in vitro* against *P. falciparum* with single-digit nanomolar activity and up to several thousand-fold lower toxicity to mammalian cells, thus demonstrating excellent selectivity (6, 7). Furthermore, it was shown to be equipotent against chloroquine- and artemisinin-resistant laboratory strains of *P. falciparum* and field isolates of *P. falciparum* and *Plasmodium vivax* (8). Pharmacokinetic studies revealed rapid microsomal clearance and low exposure *in vivo*. Nevertheless, excellent *in vivo* activity was observed in the *Plasmodium berghei* murine malaria model Peters 4-day test (8), with a 50% effective dose (ED_{50}) of 1.47 mg/kg of body weight per day for 4 days in suppressing the development of blood asexual stages of the rodent malaria. The mechanism of action of the bis-1,2,4-triazines is not known, and their unique structure,

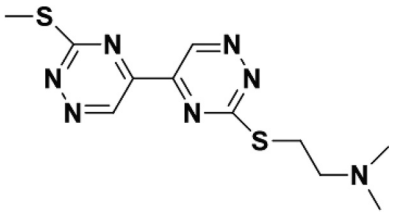

FIG 1 The representative bis-1,2,4-triazine MIPS-0004373.

compared with other known antimalarials, suggests that these compounds may act via a novel target.

In this study, MIPS-0004373 was profiled to determine its *in vitro* activity throughout the parasite life cycle and *in vivo* radical cure efficacy in the *P. berghei*-murine model. Stage specificity within the asexual *P. falciparum* life cycle, induction of parasite dormancy, transmission blocking ability, liver stage activity, and *in vivo* potency were evaluated. We demonstrated MIPS-0004373 to be active against all blood stages of the *P. falciparum* asexual life cycle and limited (predominantly early) stages of the sexual life cycle, with a fast onset of action *in vitro* and excellent *in vivo* activity in the modified Thompson test for the radical cure of *P. berghei*. The bis-1,2,4-triazine compound offers great promise for further optimization toward the development of a new medicine for the treatment of symptomatic malaria with potential for transmission-blocking activity.

RESULTS

MIPS-0004373 is highly active against all blood stages of the asexual life cycle of *P. falciparum*. The *in vitro* activity of MIPS-0004373 was determined in each of the three stages of the intraerythrocytic *P. falciparum* asexual life cycle using a pulsed-exposure format (9). Synchronized ring (3 to 6 h postinvasion [P.I.]), trophozoite (30 to 36 h P.I.), or schizont (36 to 40 h P.I.) stage parasites (3D7) were subjected to 5-h drug pulses, washed to remove the triazine compound, and returned to standard culture conditions for a further 48 to 72 h before determination of growth inhibition utilizing the SYBR green I assay. MIPS-0004373 exhibited potent activity against all parasite stages throughout the asexual life cycle of *P. falciparum*, displaying 50% inhibitory concentration (IC_{50}) values below 100 nM (Fig. 2A). The highest potency was observed in trophozoite stage parasites (IC_{50}, 28 nM), although the difference in IC_{50} values between rings, trophozoites, and schizonts was not significant ($P > 0.05$). This similar level of activity exhibited by MIPS-0004373 across the asexual blood stages differentiates the bis-1,2,4-triazines from the clinically used artemisinin- and quinoline-based antimalarials that exhibit more potent activity against the trophozoite and schizont stages (10).

The potent activity of MIPS-0004373 against trophozoites exposed to a 5-h drug pulse (IC_{50}, 28 nM) compared favorably to that of chloroquine (IC_{50}, 165 nM) (Fig. 2B), despite similar activity reported from a standard 72-h assay (6). This finding suggests a rapid onset of action, which was confirmed by the observation of substantial activity after only 1 h of bis-1,2,4-triazine exposure (IC_{50}, 170 nM) (Fig. 2B).

The bis-1,2,4-triazine inhibits progression from the ring to trophozoite stage. The activity of MIPS-0004373 across all stages of the asexual life cycle and the rapid onset of action prompted the microscopic assessment of parasite growth over the 48-h life cycle. Tightly synchronized ring stage *P. falciparum* (3D7; 3 h P.I.) was subjected to a 5-h drug pulse at 120 nM (equivalent to twice the IC_{50} of a 5-h drug pulse against ring stage parasites), then the drug was washed out and growth assessed via cultured

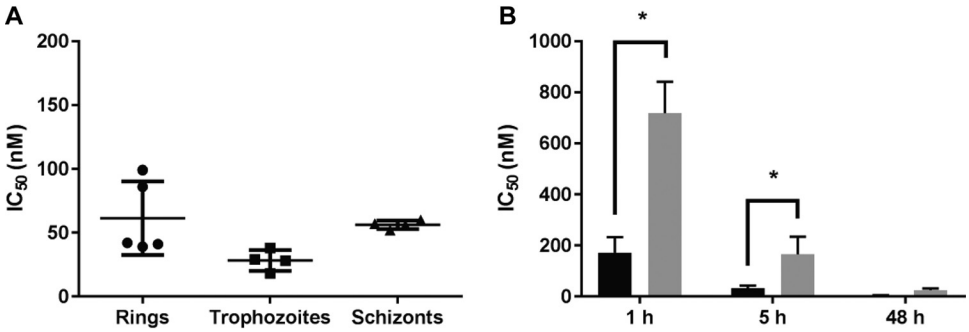

FIG 2 *In vitro* assessment of stage specificity and rate of action of MIPS-0004373 against the 3D7 strain of *P. falciparum*. (A) Asexual blood stage IC_{50} values for MIPS-0004373 against early ring stages (3 to 6 h P.I.), trophozoites (30 to 36 h P.I.), and schizonts (36 to 40 h P.I.) after a 5-h pulse. (B) IC_{50} values for MIPS-0004373 (black bars) and chloroquine (gray bars) after 1-, 5-, and 48-h drug pulses against *P. falciparum* trophozoites (30 to 36 h P.I.). Graphs show the mean ± SD, $n = 5$.

thin film microscopy at regular time points throughout the remainder of the life cycle. The addition of MIPS-0004373 had no immediate effect on the size or morphology of ring stage parasites compared with the dimethyl sulfoxide (DMSO) vehicle control (see Fig. S1 in the supplemental material). Differences between treated and untreated parasites began to appear only as the parasites transitioned into the trophozoite stage. At 16 to 18 h after the addition of MIPS-0004373 (19 to 21 h P.I.), the triazine-treated parasites demonstrated a condensed morphology. While untreated parasites continued to progress through their asexual life cycle, drug-treated parasites showed no further progression.

High bis-1,2,4-triazine concentrations arrest ring stage development *in vitro*. The young ring stage (>95% ~0 to 5 h P.I.) parasite cultures of the *P. falciparum* W2 laboratory line (parasitemia, 0.75% to 1.2%) were exposed to either high concentrations of MIPS-0004373 (1,200 nM or 150× IC_{90}) or dihydroartemisinin (DHA) (700 nM) for 6 h. The same DHA concentration and exposure time have been used in the previously published ring stage survival assay (RSA) (11, 12). The *P. falciparum* W2 line is artemisinin sensitive and fast growing, with parasites completing the asexual cycle within 36 to 40 h (13; our observation), as opposed to a 48-h cycle for *P. falciparum in vivo* or for freshly adapted cultured field isolates.

Parasite morphology and recovery after exposure to MIPS-0004373 were evaluated using cultured film microscopy and flow cytometric analysis, using either SYBR green or rhodamine 123 dyes, and they were compared with parasites exposed to DHA (700 nM) as the reference compound (14). Exposure to MIPS-0004373 arrested the progression of rings in a manner similar to what has been observed previously after exposure to DHA (12). Microscopic examination of MIPS-0004373- and DHA-treated cultures revealed similar parasite morphology, with the majority of rings appearing pyknotic with condensed nuclei in the absence of cytoplasm (see Fig. S2 in the supplemental material). Twenty-four hours after the start of the experiment, a small number of parasites demonstrated a morphology consistent with the dormant rings defined by Tucker et al. (15), accounting for 2.5% ± 0.7% for MIPS-0004373 and 4.0% ± 0.0% for DHA of the total number of ring stage parasites present on the slide. The first growing trophozoites in DHA- and MIPS-0004373-treated cultures were detected by cultured film microscopy at 72 h after starting the experiments.

In addition to cultured film microscopy analysis, the growth of parasites in untreated controls and cultures exposed to DHA or MIPS-0004373 was followed using flow cytometric analysis of SYBR green and rhodamine 123-stained parasites, with the results of one representative experiment shown in Fig. 3 and Fig. S3 and S4 in the supplemental material. Twenty-four hours after the start of the experiment, the live parasites (rhodamine 123 stained) in DHA- and MIPS-0004373-treated cultures declined to 0.03% ± 0.01% and 0.11% ± 0.01%, respectively (Fig. 3) compared with 0.95% ± 0.00% in untreated control cultures. Note that the flow cytometric analysis of SYBR green-stained parasites revealed a significant fraction of MIPS-0004373-treated rings "shifted" to the left compared with that in DHA-treated rings, which is indicative of a greater decrease in fluorescence of SYBR green (DNA-binding dye)-stained rings, presumably, resulting from DNA degradation (Fig. S3).

The parasitemia in treated cultures remained low at 48 h at a value of 0.04% ± 0.01% for both DHA- and MIPS-0004373-treated cultures. Note that by 48 h, parasitemia in the fast growing control cultures of the W2 line reached 7.1%, as judged by microscopy and SYBR green, including 1.5% of infected red blood cells (RBCs) harboring trophozoite stage parasites (Fig. S3), thus confirming progression through the 2nd asexual cycle. Note that the "live" parasite numbers were lower, presumably, because of stress on parasites caused by high parasitemia. By 72 h, the W2 line control cultures "crashed," which resulted in a further reduction in live parasites detected by rhodamine 123 staining (Fig. S4). A small increase in live parasites was detected in cultures exposed to the drugs at 72 h, namely, 0.10% ± 0.01% and 0.07% ± 0.00% in DHA- and MIPS-0004373-treated cultures, respectively. During the 168 h of follow-up, more growing parasites were observed in both drug-

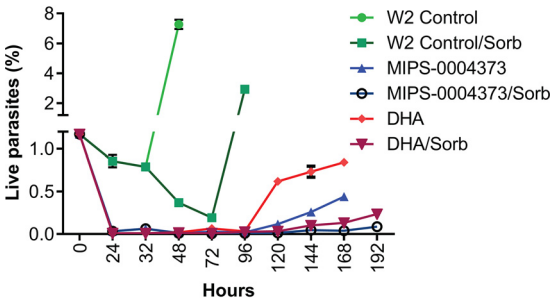

FIG 3 Live parasite dynamics following 6-h exposure to MIPS-0004373 or DHA. The live *P. falciparum* W2 parasites were detected by staining with rhodamine 123. At 32 h after the commencement of the experiment, the cultures were split and one-half was treated with 5% sorbitol (designated W2 control/sorb, MIPS-0004373/Sorb, and DHA/Sorb), whereas the other half was left untreated (designated W2 control, MIPS-0004373, and DHA). Graph shows means ± SD based on two independent experiments, with each consisting of triplicate replicates.

treated cultures; however, the recovery of MIPS-0004373-treated cultures was delayed by at least 24 h in comparison with the DHA-treated cultures (Fig. 3).

Treatment of the W2 line cultures with D-sorbitol at 32 h after the start of the experiment, when the majority of W2 control parasites were at late trophozoite and early schizont stage, was used to ascertain if the observed recovery was due to dormant parasites resuming growth or those which did not become dormant and continued to grow despite DHA or MIPS-0004373 treatment. The application of D-sorbitol in this study was similar to the removal of growing parasites by passaging through magnetic columns (12). The delay in the recovery of parasites in cultures exposed to DHA and MIPS-0004373 and subsequently treated with D-sorbitol, compared with those that were not treated, suggests that there were some parasites that were not killed or arrested and they continued to grow after drug exposure. In parasite cultures that were treated with D-sorbitol, parasite recovery was delayed by 24 h in DHA-treated cultures (from 72 to 96 h) and by 48 h in MIPS-0004373-treated cultures, from 72 to 120 h (Fig. 3).

Attempts to generate bis-1,2,4-triazine resistance *in vitro* were unsuccessful. Compounds that rapidly generate resistance-conferring mutations in *Plasmodium* sp. are not ideal clinical candidates. Determining the onset of resistance and potential resistance mechanisms are important considerations in drug development. Four independent attempts were made to generate resistance to the bis-1,2,4-triazine compound, whereby *P. falciparum* cultures were exposed to MIPS-0004373 over a 3- to 12-month period. The first two attempts subjected 3D7 strain parasites to low levels (1× IC_{50}) of MIPS-0004373 (5 nM), and the IC_{50} was monitored weekly. The first experiment resulted in no significant change in IC_{50} over a 4-month period, and parasites were unable to tolerate higher bis-1,2,4-triazine concentrations. In the subsequent attempt, it appeared that all parasites died within the first month of bis-1,2,4-triazine exposure (5 nM), and no live parasites were recovered after two more months of continuous culture. In the third attempt to generate resistance, a ramp-up method was employed (16) using the chloroquine-resistant Dd2 strain. Initially, parasites were subjected to a 2× IC_{50} concentration of MIPS-0004373 (Dd2 IC_{50}, 9 nM) and monitored daily by Giemsa-stained blood films. After three consecutive days of treatment, cultures reached a parasitemia of ~1% (starting parasitemia, ~4%) and required 4 days of compound-free media to repopulate each test flask before the next round of MIPS-0004373 exposure. This cycle continued for 27 days, after which cultures could tolerate a 3× IC_{50} concentration of MIPS-0004373 as determined by fractional increases in daily parasitemia while under compound pressure. Over a 6-month course of resistance selections, the maximum treatment concentration used was 4× IC_{50} (occurring five times), which coincided with a significant decrease in parasitemia. Bulk cultures were evaluated for resistance by dose response

TABLE 2 Select coding mutations[a] identified in Dd2 parasites exposed to MIPS-0004373 for 6 months

Flask	Clone name	Gene identifier	Gene description	Mutation type	Amino acid change
1	A9	PF3D7_0510100	KH domain-containing protein	Disruptive in-frame deletion	Ser2328_Gly2332del
		PF3D7_1471600	Conserved *Plasmodium* protein, unknown function	Missense	Asp987Tyr
	B3	PF3D7_1322100	Histone-lysine *N*-methyltransferase SET2	Nonsense	Leu884*
	D1	PF3D7_0609200	Citrate synthase-like protein	Missense	Asn39Tyr
		PF3D7_1322100	Histone-lysine *N*-methyltransferase SET2	Nonsense	Leu884*
	H8[b]				
2	D3	PF3D7_1462400	Conserved *Plasmodium* protein, unknown function	Nonsense	Tyr2603*
	D12	PF3D7_1008100	PHD finger protein PHD1	Missense	His1762Tyr
		PF3D7_1456500	STAG domain-containing protein	Missense	Thr66Ala
		PF3D7_1462400	Conserved *Plasmodium* protein, unknown function	Nonsense	Tyr2603*
	F8[b]				
	H1	PF3D7_1459200	WD repeat-containing protein	Frameshift	Val359fs
3	B11	PF3D7_1322100	Histone-lysine *N*-methyltransferase SET2	Nonsense	Leu884*
	C9	PF3D7_1205500	Zinc finger protein	Missense	Trp678Leu
	F1[b]				
	H6	PF3D7_1322100	Histone-lysine *N*-methyltransferase SET2	Nonsense	Leu884*

[a]The full set of mutations are provided in Data Set S1.
[b]Had no coding mutations of interest.

assays (IC_{50}) every 2 to 3 weeks. However, no stable change to the IC_{50} of MIPS-0004373 was observed. The fourth attempt used a similar stepwise method, starting with a different Dd2 clone and a 1× IC_{50} concentration (IC_{50}, 13 nM), with 10% concentration increments when tolerated (see Fig. S5 in the supplemental material). Again, no significant increase in IC_{50} of MIPS-0004373 was observed for any of the three replicate flasks over the 12-month period, with the IC_{50} values remaining within 30% of the initial clone. The maximum treatment concentration which allowed recovery (after significant parasite killing) was 2.8× IC_{50} (37 nM), indicating that none of these attempts were successful at generating bis-1,2,4-triazine-resistant parasites.

In addition, no substantial increase in IC_{50} was observed when one of the drug-selected lines (attempt 4, replicate 2 [rep2]) was tested in a ring stage survival assay (Fig. S5F). In this assay of 0- to 3-hour postinfection rings, an IC_{50} of 240 ± 18 nM was observed for a 6-h pulse of MIPS-0004373 compared with an IC_{50} of 128 ± 23 nM for the parental Dd2 strain. This average 1.89-fold decrease in activity is comparable to that observed for a standard 48-h assay. Furthermore, no obvious difference in maximal killing was observed at high doses, indicating that no unique ring stage resistance—such as that associated with artemisinins—was observed for MIPS-0004373.

To detect variants that may have evolved over the treatment period, four clones from each of the three flasks from the third attempt were isolated and sent for whole-genome sequencing. While there were no common mutated genes observed across all clones, it was notable that many of the mutations occurred in genes encoding nuclear proteins involved in epigenetic processes, such as the histone-lysine *N*-methyltransferase SET2 (PF3D7_1322100) (Table 2; see Data Set S1 in the supplemental material).

MIPS-0004373 displays limited transmission-blocking potential with the greatest potency against male gametocytes. The activity of MIPS-0004373 against the sexual stages of the *P. falciparum* life cycle was assessed to determine the transmission-blocking potential of the bis-1,2,4-triazine. The compound was tested for speed of action against gametocytes, stage-specific inhibition of gametocytes, and inhibition of female and male gamete formation. The speed of action of bis-1,2,4-triazines against gametocytes at various stages of development was analyzed using the luciferase time to kill assay. Ring stage (day 0) and mature stage V (day 12) $NF54^{Pfs16}$ strain gametocytes were incubated with MIPS-0004373 for 6 h (ring stages only), 24 h, 48 h, and 72 h (Fig. 4), followed by measurement of luciferase activity as previously described (17, 18). This activity was then confirmed using the imaging-based stage-specificity study, by incubating ring stage (day 0), early stage (day two), late stage (day eight), and mature stage

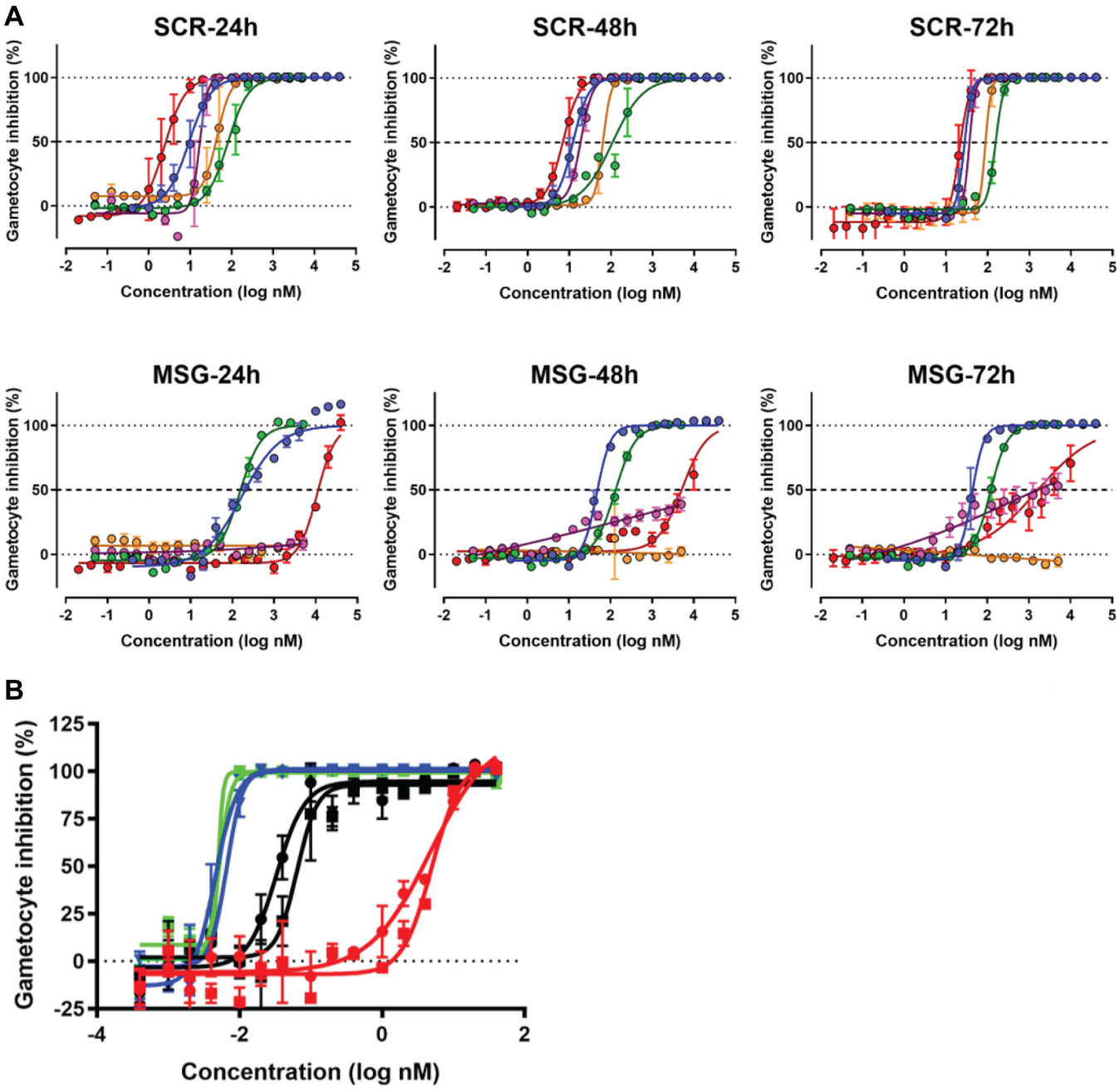

FIG 4 Activity and speed of action of MIPS-0004373 against gametocytes. (A) Sexually committed rings (SCR) and mature stage gametocytes (MSG) were exposed to the compound for 24, 48, or 72 h, and gametocyte inhibition was analyzed by luciferase activity. IC_{50} curves for MIPS-0004373 (red), methylene blue (blue), puromycin (green), chloroquine (yellow), and artemisinin (pink). Puromycin was included as the positive control. Two independent experiments are displayed, with each consisting of two replicates. (B) The bis-1,2,4-triazine potently inhibits sexually committed rings, although it has low activity on mature gametocytes. IC_{50} curves for sexually committed rings (green), day 2 early stage gametocytes (blue), day 8 late stage gametocytes (black), and day 12 MSG (red). Data show the means ± SEM of two biological replicates with two technical replicates.

(day 12) gametocytes with the compound for 48 h, followed by imaging of the plates as previously described (19). MIPS-0004373 displayed potent inhibition of sexually committed ring stage parasites with an IC_{50} below 22 nM in both the luciferase and imaging assays. This result indicates a potency similar to that observed for artemisinin and methylene blue and greater activity than chloroquine against sexually committed rings (Fig. 4A).

The bis-1,2,4-triazine showed a fast onset of action, with killing observed after just 24 h of treatment against both ring stage and mature gametocytes. However, as

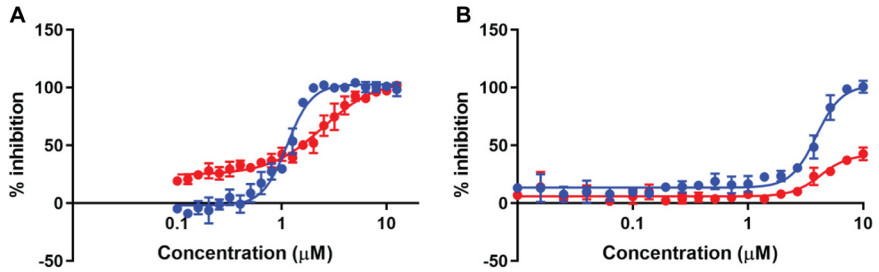

FIG 5 Bis-1,2,4-triazine activity in late stage male and female gametocytes. IC_{50} curves for the control compound Gentian violet (A) and MIPS-0004373 (B) in male gametocytes (blue) and female gametocytes (red). Data show the means ± SD of one biological experiment with four replicates.

gametocytogenesis progressed, MIPS-0004373 showed a gradual decrease in activity. This finding was confirmed by the imaging stage assay where MIPS-0004373 activity was highest up to stage II of gametocytogenesis, with an IC_{50} of 5.6 nM. The activity then declined as gametocytogenesis progressed; a 9-fold lower IC_{50} of 49 nM was observed against stage IV gametocytes (Fig. 4B). The luciferase assay confirmed the reduced potency of MIPS-0004373 against stage IV parasites (IC_{50}, 200 nM). Mature stage V gametocytes appeared largely insensitive to the compound with an IC_{50} of >5 μM after a 48-h incubation period. When tested in the acridine orange female gamete formation assay (16), the compound did not inhibit the formation of female gametes up to a concentration of 20 μM.

The stage-specific activity of MIPS-0004373 was confirmed using the gametocyte high-content imaging assay (20). Here, efficacy against specific stages of intraerythrocytic gametocytes was determined after 72 h of incubation with MIPS-0004373, using puromycin and DMSO as the positive and negative control, respectively. This assay confirmed potent activity against younger gametocytes, with >80% reduction in stage I to III counts at MIPS-0004373 concentrations above 154 nM (see Fig. S6 in the supplemental material). The broadened concentration response slope in stages IV to V suggest waning sensitivity to mature forms. Interestingly, significant activity was still observed against mature gametocytes (stage V) with an IC_{50} of 255 ± 169 nM in this assay; however, a bottom plateau in the dose-response curve was missing, with maximal gametocytocidal effect (100% inhibition) resulting only at 12.5 μM. This value remains significantly less potent than the 1 μM threshold that is used commonly to signify gametocytocidal activity.

The activity of the bis-1,2,4-triazine on male and female late stage gametocytes was tested using the dual gamete formation assay (21, 22). It has previously been shown that male gametocytes are more susceptible to a wide range of antimalarial compounds than female gametocytes (21). Furthermore, the ratio of gametocytes is generally female biased (~3 to 5 females: 1 male), meaning non-sex specific assays may miss compounds that specifically inhibit male gametocytes or male gamete formation. MIPS-0004373 showed low micromolar activity in the male exflagellation assay (3.9 μM) and very slight activity against female gametocytes (>25 μM) (Fig. 5). Complete parasite inhibition was achieved at the highest concentration of 25 μM for male gametocytes, demonstrating weak activity against the male transmission-specific forms of the parasite.

Liver stages demonstrate species-specific susceptibility to bis-1,2,4-triazine treatment. The activity of MIPS-0004373 was also assessed in the *P. berghei* liver stage assay, adapted from Swann et al. (23), which is based on the murine *P. berghei* species transfected to express firefly luciferase. This assay allows for the identification of compounds with activity against the sporozoite infection of liver cells as well as those that decrease the viability of liver schizonts. MIPS-0004373 demonstrated potent liver stage activity in this assay (IC_{50}, 199 nM; 95% CI, 146.5 to 267.2 nM), with 100% parasite inhibition observed at ≥5.55 μM (Fig. 6A). A counterscreen with uninfected HepG2 cells was performed simultaneously to measure the potential cytotoxicity of MIPS-0004373 on host liver

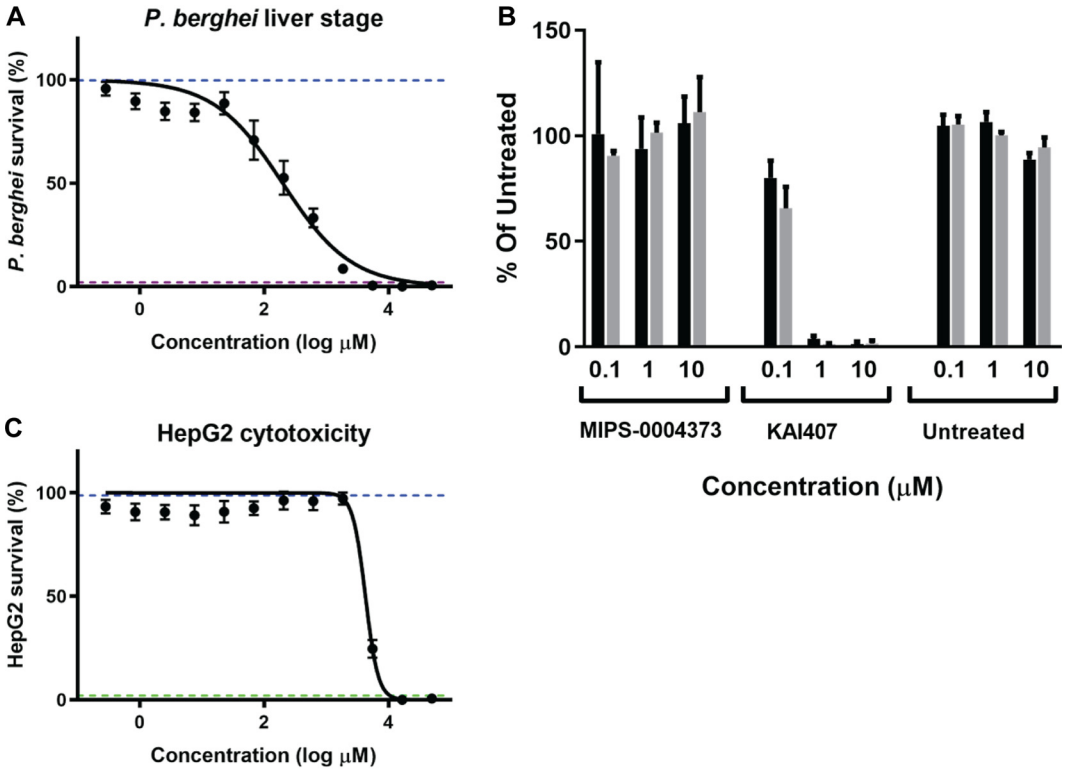

FIG 6 *In vitro* chemoprotective effect of MIPS-0004373 against liver stage parasites. (A) Freshly dissected *P. berghei* sporozoites expressing luciferase were dispensed onto HepG2 hepatocytes pretreated with increasing concentrations of MIPS-0004373. Activity was determined from the bioluminescence of viable parasites after 48 h of incubation, during which MIPS-0004373 (black circle) acted in a dose-dependent manner. Average survival (%) of extraerythrocytic forms (EEFs) is shown against atovaquone (1 μM; purple dashed line) and DMSO (0.5%; blue dashed line). (B) Uninfected HepG2 hepatocytes showed susceptibility to MIPS-0004373 (black circle) at $\geq$5.55 μM but remain largely insensitive at concentrations relevant to an antimalarial effect. Average HepG2 survival (%) is shown with puromycin (5 μM; green dashed line) and DMSO (0.5%; blue dashed line). These data represent three biological replicates against *P. berghei* liver stages and four biological replicates in the HepG2 cytotoxicity evaluation (error bars = SEM). (C) Three-point 10-fold dilution series (0.1, 1, and 10 μM) for MIPS-0004373 activity against *P. cynomolgi* liver stage cultures. The percentage of untreated control is shown as a function of test compound concentration. Differential counting of schizonts and hypnozoite forms was performed based on the size and number of parasite nuclei. The results of three assays are shown. KAI407 is included as a positive control known to have a liver stage activity profile similar to that of primaquine (44), and the untreated samples are vehicle controls (DMSO). Small liver stage forms are represented by the dark bars and large forms by the light bars.

cells, using puromycin (5 μM) and DMSO (0.5%) as positive and negative controls, respectively. Compounds with a 10-fold or greater potency against *P. berghei* liver stage development versus uninfected HepG2 cells can be considered to be specific for the parasite. The average IC_{50} of MIPS-0004373 in HepG2 was 4.27 $\pm$ 0.099 μM (Fig. 6A), suggesting the potent activity against *P. berghei* exoerythrocytic forms is not a function of host cell toxicity.

To further investigate liver stage activity, the *in vitro Plasmodium cynomolgi* liver stage culture platform (21) was utilized to determine the activity of MIPS-0004373 in a primate malaria model closely related to *Plasmodium vivax*. *P. cynomolgi* is one of the few parasite species that produces hypnozoites analogous to those of *P. vivax*. Previous work has found that two populations of parasites could be identified from primate livers infected with *P. cynomolgi*, namely, small forms that resemble hypnozoites and large forms that resemble developing liver stage schizonts (21). MIPS-0004373 showed no activity against either *P. cynomolgi* small or large liver stage forms, even at the highest tested concentration of 10 μM (Fig. 6C).

The *in vitro* antimalarial activity profile of MIPS-0004373 that was generated in this study covers various stages of the complex *P. falciparum* life cycle. This compound represents an exciting new antimalarial series with potency in all asexual blood stage

TABLE 3 Summary of MIPS-0004373 activity across the complex *P. falciparum* life cycle

Species	Assay	IC_{50} data of asexual stage parasites from liver and blood cycles (nM)[a]					Figure or reference
		Liver stage	Ring	Trophozoite	Schizont	Asynchronous stages	
P. cynomolgi	Hypnozoite inhibition	>10 000					6A
P. berghei	48-h IC_{50} survival assay	199 (46.5–267.2)[b]					6B
P. falciparum	3D7 1-h pulse IC_{50} survival assay			171 ± 62			2B
	3D7 5-h pulse IC_{50} survival assay		61 ± 29	28 ± 8, 32 ± 11	56 ± 3		2A, 2B
	3D7 48-h IC_{50} survival assay			4 ± 1			2B
	3D7 72-h IC_{50} survival assay					8 ± 4	6

[a]Values show the mean ± SD of at least three biological replicates with at least two technical repeats.
[b]95% confidence interval.

parasites (Table 3) and a potential to evaluate future analogues for liver stage and transmission blocking activity (Table 4).

MIPS-0004373 effectively clears *P. berghei* infection *in vivo*. The *in vivo* efficacy of MIPS-0004373 was evaluated in the modified Thompson test (24) over a dose range of 2 to 64 mg/kg/day for 3 days against an established murine infection of *P. berghei*. The bis-1,2,4-triazine was well tolerated in mice up to the targeted dose of 64 mg/kg/day for 3 days with no observed physical adverse events, such as loss of mobility, poor posture, and ruffled fur coat. MIPS-0004373 cleared a mean starting *P. berghei* parasitemia of 2.14% (range, 1.02% to 3.26% for the three groups of mice treated with 64 mg/kg/day of the bis-1,2,4-triazine) in about 3 days, which was similar to the speed of action of chloroquine but slightly slower than that of artesunate given the same dose of 64 mg/kg/day for 3 days (Table 5). Lower doses of MIPS-0004373 did not clear the *P. berghei* infections. Daily monitoring of the mice after parasite clearance revealed recrudescences to occur at about day 5 in animals treated with artesunate. In contrast, mice treated with either MIPS-0004373 or chloroquine recrudesced about 8 days after commencement of treatment. Of note, one mouse with a parasitemia of 1.9% before commencement of treatment with 64 mg/kg/day of MIPS-0004373 was still blood film negative at day 31 of follow-up and was deemed to have been cured of the *P. berghei* infection. These findings show that the efficacy of MIPS-0004373 in the modified Thompson test is comparable to that of chloroquine and provides evidence that MIPS-0004373 has a killing effect similar to that of both artesunate and chloroquine.

DISCUSSION

The management of malaria currently relies heavily on the use of ACTs for the treatment of acute *P. falciparum* malaria. Recent reports of resistance to ACTs, such as dihydroartemisinin-piperaquine (25, 26), have emphasized the need to discover new antimalarial medicines with novel mechanisms of action. Excitingly, some novel antimalarial chemotypes have recently entered clinical trials. However, the drug development process is known to be affected by attrition which, combined with the inevitable development of antimicrobial

TABLE 4 Summary of MIPS-0004373 activity of sexual stage *P. falciparum*

Assay	IC_{50} data (nM)[a]						Figure
	Committed ring	Stage II gametocyte	Stage IV gametocyte	Mature stage V gametocyte	Male	Female	
NF54 24-h time-to-kill assay	3 ± 1			>1,000			4A
NF54 48-h time-to-kill assay	8 ± 3			4,514 ± 1,635			4A
NF54 72-h time-to-kill assay	22 ± 5			1,997 ± 1,335			4A
72-h NF54 high-content imaging assay	5 ± 0.1	6 ± 1	49 ± 15	255 ± 169			4B
Dual gamete formation assay					3,903 ± 184[b]	> 25,000[b]	5
AO female gamete assay						>20,000	

[a]Data show the means ± SEM of two biological replicates with two technical replicates.
[b]Mean ± SD of one biological experiment with four replicates.

TABLE 5 *In vivo* efficacy of MIPS-0004373, artesunate, and chloroquine against established *P. berghei* infection in the modified Thompson test

Parameter	Treatment[a]	Expt 1	Expt 2	Expt 3
Starting parasitemia[b] (%) for treatment at D0		1.68 (0.54–3.26)	1.68 (1.43–2.13)	1.65 (1.02–2.23)
Day of parasite clearance after starting treatment	MIPS-0004373	D + 3	D + 4	D + 2
	Artesunate	D + 3	D + 2	D + 2
	Chloroquine	D + 3	D + 3	D + 3
Day of recrudescence after starting treatment	MIPS-0004373	D + 8	D + 7	D + 8
	Artesunate	D + 5	D + 5	D + 4
	Chloroquine	D + 8	D + 8	D + 8

[a]Dose was 64 mg/kg/day × 3.
[b]Mean (range) parasitemia values based on flow cytometry for the drug-treated and vehicle control groups of mice. $n = 6$ mice per group.

resistance, highlights the need to discover and develop new antimalarial chemotypes. In addition, the push toward an elimination and eradication agenda for malaria has gained momentum in recent years, and these ambitious goals will require a range of antimalarials with activity against different stages of the parasite in order to effectively eliminate the spread of disease. The MMV has outlined a range of target candidate profiles with lists of requirements that are necessary to address these specific needs, as described above (Table 1).

In vitro activity assays identified MIPS-0004373 to be fast acting and potent against all three studied stages of the parasite asexual life cycle. Importantly, the excellent potency observed against all asexual stages differentiates the bis-1,2,4-triazines from other currently used antimalarials, providing a potential alternative to artemisinins and an advantage over the currently used quinoline-based compounds (10). The combined potent activity of MIPS-0004373 against ring stage asexual parasites and early stage gametocytes is distinct from currently approved antimalarials and suggests that bis-1,2,4-triazines act by a different mechanism of action. Attempts to generate robustly resistant parasites in order to study potential mechanisms of action and resistance were unsuccessful, although the identification of multiple mutations in epigenetic genes in the parasite clones exposed to MIPS-0004373 over a 6-month period could provide some general clues to the pathway(s) involved in the triazine parasite-killing mechanism. It is possible that the observed mutations provide additional tolerance to the compound without conferring a true resistance phenotype, as detected by standard dose-response methods. Alternative approaches are necessary to fully elucidate the mode of action. Nevertheless, the inability to select for robust resistance against this potent bis-1,2,4-triazine compound (MIPS-0004373) after >2 years of cumulative exposure is a promising attribute for future clinical development and usage (16). It has been shown previously that fast-acting compounds have a lesser tendency for developing *de novo* resistance. Sanz et al. observed a positive correlation between fast onset of action and the inability to generate resistance (16, 27). This observation agrees with the results for MIPS-0004373 in the activity assays. Fast-acting compounds have many benefits, including rapid clearance of parasites, the ability to alleviate symptoms quickly, and, as mentioned, limiting the development of resistance (16). It has also been suggested that the nature of the target may be responsible for cases where resistance could not be generated, for example the target gene having mutational flexibility or the possibility that the compound inhibits several targets (16).

When tested in the rodent *P. berghei* modified Thompson test for radical cure, MIPS-0004373 was as potent as artesunate and chloroquine in clearing an established infection of *P. berghei* by 72 h after commencing oral treatment with 64 mg/kg/day over 3 days. Recrudescence occurred around 8 days after the commencement of MIPS-0004373 treatment, which is comparable to that for chloroquine, but demonstrates a killing effect similar to that of both artesunate and chloroquine. This extended activity

of MIPS-0004373 is somewhat surprising given that pharmacokinetic studies have shown that MIPS-0004373 is cleared rapidly *in vivo* (8) and may implicate prolonged exposure of an active metabolite and/or superior reduction of parasitemia immediately following drug exposure. Interestingly, although the *in vitro* ring stage survival assay revealed the presence of some rings with morphology that may indicate the induction of dormancy, similar to those observed following DHA treatment, it did demonstrate a longer time to recrudescence for MIPS-0004373 than that for DHA, which may suggest more efficient parasite killing by MIPS-0004373 even after a short 6-h period of exposure. Overall, the kinetics of antiparasitic activity *in vitro* and *in vivo*, and the inability to select for resistance *in vitro* (to date), support further development of the bis-1,2,4-triazine series to identify a lead candidate for the treatment of symptomatic malaria (TCP-1).

MIPS-0004373 displayed no activity against dormant liver stage *P. cynomolgi* hypnozoites and is therefore not suitable for relapse prevention (TCP-3). The *in vitro* infection of rhesus hepatocytes by *P. cynomolgi* sporozoites is considered the gold standard for measuring hypnozoite inhibition. However, the disadvantage of this method is the species difference of parasite and host cells. MIPS-0004373 also showed no activity against hepatic schizonts in the *P. cynomolgi* assay but revealed an IC_{50} of 199 nM against *P. berghei* liver stages. This finding may indicate species-specific differences in the susceptibility of the liver stage parasites or may suggest activity against the process of invasion and initial infection of hepatocytes in the *P. berghei* model but an inability to clear established infection in the *P. cynomolgi* model. It would be highly beneficial to discover an attractive TCP-4 molecule that displays activity against hepatic schizonts or casual liver stage activity, in order to provide chemoprotection. While the lack of activity against *P. cynomolgi* liver stages indicates that the current series of bis-1,2,4-triazines is not suitable as a TCP-4 molecule, further investigations of the chemoprotective potential of this series are warranted. New assays have been developed recently for the analysis of the liver stages of malaria, such as micropatterned primary human hepatocyte cocultures (28), and it is anticipated that the next generation of bis-1,2,4-triazines could be tested in these alternative assays to further interrogate the liver stage activity in different parasite and host cell models.

MIPS-0004373 displayed potent activity against sexually committed ring stage parasites, similar to that observed for artemisinin and methylene blue (Fig. 4), and was more active than chloroquine. The bis-1,2,4-triazine demonstrated a fast onset of action against both ring stage and mature gametocytes, with growth inhibition observed after 24 h of treatment. The observed onset of action is similar to that of artemisinin and methylene blue, suggesting MIPS-0004373 has activity against sexual stage parasites that is comparable to the current first-line treatments. The inhibition of late stage gametocytes is a requirement of TCP-5 molecules in order to prevent transmission from the human host to the mosquito vector. Based on this criterion, MIPS-0004373 cannot be classified as a TCP-5 molecule, but the low level of activity suggests that further optimization may lead to the discovery of bis-1,2,4-triazine analogues that adequately target this stage. It has been shown that multiple compounds display far greater activity against male stage V gametocytes than those for female gametocytes (21), and MIPS-0004373 follows this trend. It appears that enhanced activity against mature female gametocytes is needed for the bis-1,2,4-triazines to effectively block transmission (TCP-5).

This study has demonstrated the suitability of bis-1,2,4-triazine antimalarials to be further investigated for their clearance of asexual blood stage parasitemia (TCP-1). Further advancement of the bis-1,2,4-triazine series will focus on optimization of the pharmacokinetic and toxicity profile, while maintaining the excellent antiparasitic potency. The stage-specific and sex-specific activity against gametocytes and the species-specific activity against liver stage schizonts should be reassessed with the next generation of bis-1,2,4-triazines to determine whether preventative or transmission-blocking activity are feasible with this pharmacophore. It will be important to investigate the mechanism of action by which bis-1,2,4-triazine compounds inhibit *P. falciparum* parasite growth, as the identification of the protein target will allow for structure-based

design and for optimal selection of combination regimens to be developed for future clinical usage.

Overall, the bis-1,2,4-triazine compounds have the potential to be further developed for the treatment of uncomplicated malaria. Their fast onset of action against all asexual blood stages, sustained suppression of parasitemia *in vivo*, and inability to easily select for resistance are all attractive properties of these bis-1,2,4-triazine compounds.

MATERIALS AND METHODS

Culturing and tight synchronization of parasites. Asexual *P. falciparum* 3D7 parasites were cultured under standard conditions (29) with minor modifications, using RBCs (Australian Red Cross Blood Service) at 2% hematocrit in modified RPMI 1640 medium (10.4 g/liter), HEPES (5.94 g/liter), hypoxanthine (50 mg/liter), $NaHCO_3$ (2.1 g/liter), and Albumax (5 g/liter) at 37°C under a defined atmosphere (carbogen, 95% N_2, 4% CO_2, and 1% O_2). Parasites were synchronized routinely with 5% (wt/vol) D-sorbitol (30). Synchronization and parasitemia were assessed by light microscopic evaluation of Giemsa-stained thin blood films (>500 parasites counted per slide), and the hematocrit was determined by counting cells with a Brightline counting chamber hemocytometer (LW Scientific).

To generate tightly synchronized 3D7 parasites (31), multiple rounds of sorbitol treatments were performed. Cultures were tightly synchronized to a 2- to 3-h window with two sorbitol treatments performed within 14 to 16 h of each other. When mature schizonts began to burst and the ring:schizont ratio was greater than 2:1, a third sorbitol treatment was performed.

48-h growth inhibition assay using SYBR green I. The antimalarial activity of the bis-1,2,4-triazine compound was determined using a standard drug sensitivity assay (32) by exposing parasites to a drug dilution series (concentrations ranging from 0.25 nM to 200 nM) for 48 h in a 96-well plate format. Briefly, stock solutions of the test compounds prepared in DMSO (1 mM) were first diluted with complete RPMI medium and then serially diluted with medium in a flat-bottomed 96-well plate to achieve a final volume of 50 μl in each well. An equal volume of parasites was then added to each well to achieve a final parasitemia of 0.5 to 1% and hematocrit of 2% in 100 μl of culture medium. Samples maintained under lethal MIPS-0004373 drug pressure (>200 nM) for 48 h acted as the control for 100% parasite killing, and infected RBCs incubated without drug acted as the control for 100% parasite growth. Parasite cultures were incubated for 48 h at 37°C under an atmosphere of 1% O_2, 5% CO_2, and 94% N_2.

After the 48-h incubation period, parasite drug susceptibility was assessed by the SYBR green assay, as previously described (32). Briefly, the culture medium in each well was refreshed, and 100 μl of lysis buffer containing 0.1 μl/ml of SYBR green I was added. The contents of the well were mixed until no RBC sediment remained, and the plates were incubated for 1 h in the dark at room temperature. Fluorescence was then measured on an EnSpire plate reader (Perkin Elmer) with excitation and emission wavelengths of 485 nm and 530 nm, respectively, and a gain setting of 50 (32, 33). Data analysis was performed using GraphPad Prism (San Diego, CA) software by plotting the fluorescence values against the logarithm of the drug concentration and normalizing by the mean fluorescence intensities for the 100% growth and killing control wells. Curve fitting was performed using the sigmoidal 4 parameter logistic regression (4PL) function to determine the drug concentration that produced 50% growth inhibition (IC_{50}) relative to the drug-free control wells. Experiments were performed with triplicate technical replicates in at least two independent experiments.

***In vitro* stage-specificity assays for asexual blood stage *P. falciparum*.** The drug pulse parasite viability assay method was adapted from a previously described method (9). Drug stocks were prepared in fresh RPMI medium and serially diluted with complete RPMI medium in round-bottom 96-well microtiter plates. Cultures of infected RBCs (iRBCs) and uninfected RBCs (uRBCs) were adjusted to achieve a final hematocrit of 1% to 2% and iRBC cultures were adjusted to 0.2% parasitemia. Plates were then incubated for 1 h or 5 h at 37°C under an atmosphere of 1% O_2, 5% CO_2, and 94% N_2. Following the 5-h drug incubation period, cultures were washed three times with 200 μl of complete medium. Cultures were then incubated at 37°C under an atmosphere of 1% O_2, 5% CO_2, and 94% N_2 until assessment of parasitemia (~48 h for trophozoite and schizont stage assays, and slightly longer [~72 h] for ring stage assays to ensure highly sensitive analysis of mature parasites at the time of assessment). Samples maintained under lethal MIPS-0004373 drug pressure (>200 nM) for 48 h acted as the 100% parasite killing control, and iRBCs incubated without drug compound acted as the 100% growth control. After lysis, well contents were transferred to a flat-bottom 96-well plate for the measurement of fluorescence with SYBR green I as described above.

Microscopic assessment of growth. Synchronized ring stage (3 h P.I.) *P. falciparum* was treated with MIPS-0004373 (120 nM) or vehicle (DMSO) control and incubated for 5 h at 37°C under an atmosphere of 1% O_2, 5% CO_2, and 94% N_2. Following the 5-h drug incubation period, cultures were washed three times with complete medium. Cultures were then incubated at 37°C under an atmosphere of 1% O_2, 5% CO_2, and 94% N_2 until assessment of parasitemia. Growth assessment was performed at 10, 16, 18, 20, 22, 24, 26, and 42 h after drug addition, by Giemsa staining and light microscopy.

Ring stage survival assay and dormancy assessment. *P. falciparum* W2 parasites were maintained as described above and synchronized routinely with D-sorbitol. For the dormancy experiments, an additional synchronization with heparin was carried out prior to the experiment (34). Heparin (Pfizer, Australia) was added to culture (2 U/ml of culture) at the late trophozoite to early schizont stage to prevent newly released merozoites from invading RBCs. When cultures reached the mature schizont stage, they were centrifuged at 500 $\times$ *g* for 5 min, resuspended in complete medium, and incubated at 37°C at

90% N_2, 5% CO_2, and 5% O_2 for an additional 3 h. Following incubation, the cultures were treated with D-sorbitol to remove remaining schizonts. This process resulted in highly synchronous cultures, typically >95% of parasites at the early ring stage (≤3 h P.I.).

Young ring (0 to 3 h P.I.) parasite cultures (3 ml or 6 ml) at 0.75% to 1.2% parasitemia and 4% hematocrit were exposed to MIPS-0004373 (1,200 nM; ~150× IC_{90} for W2) and to the reference drug DHA (stock prepared to 1 mM in 100% methanol) at 700 nM for 6 h under normal growth conditions. The concentration of DHA (700 nM) used in the present study was in accordance with dormancy studies of the W2 *P. falciparum* strain as previously described by Teuscher et al. (12) and Witkowski et al. (35). Following incubation, the drugs were removed by three washes with medium, resuspended in the original volume of complete medium, and incubated at 37°C under normal growth conditions. Three experiments were performed. In the second and third experiments, parasite cultures were split in halves, with one-half (3 ml) treated with 5% D-sorbitol for 5 min at 30 h from the beginning of drug exposure and the other half left untreated. The D-sorbitol exposure ensures the removal of those parasites that had not become dormant but continued to grow. After sorbitol treatment, the cultures were plated in triplicates into the 96-well plates and monitored for parasite growth by microscopy and flow cytometry for 7 to 8 days. For flow cytometry analysis, samples (in triplicates) were stained with either the fluorescent nucleic acid intercalating dye SYBR green (Invitrogen, Australia) or the mitochondrial vital dye rhodamine 123 and then quantified by flow cytometry (FC500; Beckman Coulter, Australia). SYBR green preferentially binds to parasitic nucleic acids and is a measure of parasitic growth, but it does not allow for the distinction between dead and growing parasites. In contrast, the uptake of rhodamine 123 is dependent on the negative mitochondrial membrane potential and is indicative of parasite viability (36).

Ring stage survival assays for the MIPS-0004373-selected strain (resistance attempt 4, replicate 2) (Fig. S5F) and the parent $Dd2_{clone2}$ strain were completed in tandem as described above with minor modifications. Briefly, segmented schizonts were magnet harvested and left to invade fresh uRBCs before treatment with 5% (wt/vol) D-sorbitol 3 hours later to achieve cultures containing only young (0 to 3 h P.I.) ring stage parasites. Cultures at 1% parasitemia and 2% hematocrit were exposed to a dilution series of MIPS-0004373 starting at 700 nM for 6 h under normal growth conditions. Following incubation, the drug was removed by three washes with medium, resuspended in the original volume of complete medium, and incubated at 37°C under normal growth conditions for a further 66 h. Afterward, the activity (RSA_{0-3h} survival rate [%]) was analyzed using the SYBR green I assay as described above. Three experiments were performed with two technical replicates.

Method for development of resistance. In the first two attempts, 3D7 strain parasites were subjected continually to low levels (1× IC_{50}) of MIPS-0004373 (5 nM). Parasite cultures were maintained as described above, and the activity (IC_{50}) was monitored weekly (if parasites were present) using the SYBR green I assay described above. Selections occurred over 91 and 125 days. When parasites were growing well under these conditions, a separate dish was prepared with the drug concentration increased to 10 nM; however, parasites did not survive after three life cycles under these conditions.

In the third and fourth attempts, three independent replicates of a clonal *P. falciparum* Dd2 parent population (~1×10^9 parasites per replicate) were subjected to increasing concentrations of MIPS-0004373. Cultures were tracked daily by Giemsa-stained blood films and maintained using similar methods to those outlined for 3D7 above. When parasitemia fell below 1% to 1.5%, cultures were treated with compound-free media and allowed to recrudesce. In order to measure for resistance in each replicate, MIPS-0004373 was tested in dose response as previously described (37). In the third attempt, the primary exposure started at 2× IC_{50} ($Dd2_{clone1}$ IC_{50}, 8.75 ± 2.8 nM) and never exceeded 4× IC_{50} over 186 days. In the fourth attempt, the primary exposure started at 1× IC_{50} ($Dd2_{clone2}$ IC_{50}, 13 nM) and never exceeded 2.8× IC_{50} over 365 days. After termination of the selection experiment, four clones were isolated from each of three flasks through limiting dilution and sent for whole-genome sequencing.

Whole-genome sequencing and analysis. Genomic DNA (gDNA) was obtained from MIPS-0004373-selected parasite samples (four clones isolated from each of three flasks in the third attempt described above) by washing infected RBCs with 0.05% saponin and using the DNeasy blood and tissue kit (Qiagen) following standard protocols. Sequencing libraries were prepared by the UCSD Institute for Genomic Medicine (IGM) Genomics Center using the Nextera XT kit (catalog [cat.] no FC-131-1024, Illumina) with 2-ng input gDNA and standard dual indexing. Libraries were sequenced on the Illumina HiSeq 2500 platform (paired end 100 [PE100], RapidRun mode) to an average of 49× mean whole-genome coverage (Table S1).

Sequencing reads were aligned to the *P. falciparum* 3D7 reference genome (PlasmoDB v13.0) and preprocessed following a previously described pipeline (38). Mutations were called using GATK HaplotypeCaller, filtered by quality according to GATK recommendations (39, 40), and annotated with SnpEff (41). Finally, mutations that were present in both the compound-exposed clones and the nonexposed Dd2 parent line were removed so that mutations in the final variant calling data set were retained only if they arose during the course of treatment with MIPS-0004373.

Luciferase gametocyte assay (time to kill study) and AO female gamete formation assay. *P. falciparum* 3D7A and $NF54^{Pfs16}$ asexual stages were grown in RPMI 1640 supplemented with 25 mM HEPES, 5% AB human male serum, 2.5 mg/ml Albumax II, and 0.37 mM hypoxanthine. Gametocytes were obtained by standard induction methods, described earlier (42). Gametocytes at various stages of development were exposed to the experimental compound in 384-well luciferase (Optiplate; PerkinElmer) or imaging (CellCarrier; PerkinElmer) microplates as previously described (17–19, 43). Artemisinin, chloroquine, dihydroartemisinin, methylene blue, puromycin, pyronaridine, and/or pyrimethamine were used as reference compounds. Puromycin 5 μM and 0.4% DMSO were used as positive and negative controls, respectively. A 10 mM stock solution of the compound in 100% DMSO was diluted in water (1:25) and

culture (1:10) to a final DMSO concentration of 0.4%. Chloroquine stock solution was prepared in water and diluted as the other compounds. All the compounds were tested in either 16-concentration or 21-concentration full-dose response, using 3 concentrations per log dose. All sample and control wells contained the same final amounts of solvents. Plates were incubated with compounds at 90% N_2, 5% CO_2, and 5% O_2. Readout data were normalized to positive and negative controls to obtain % inhibition data, which were then used to calculate IC_{50} values, through a 4-parameter logistic curve fitting function in GraphPad Prism.

The compound was tested for speed of action against gametocytes at different times of development. Ring stage and mature stage V *P. falciparum* NF54^{Pfs16} gametocytes on day 0 and day 12 of gametocytogenesis, respectively, were incubated with compounds for 6 h (ring stages only), 24, 48, and 72 h. After the incubation, the luciferase activity was measured as previously described (17, 18). A 0-h incubation luciferase artifact test was also carried out on sexually committed rings to rule out an artifactual direct inhibition of the luciferase enzyme. In addition, the compound was tested for female gamete formation by exposing mature stage V gametocytes on day 12 of gametocytogenesis to the compound for 48 h, followed by staining with acridine orange and activation with xanthurenic acid, as previously described (19). The experiment was carried out in two independent experiments, with each consisting of two replicates.

Gametocyte high-content imaging assay. Stage-specific gametocytes were generated using previously described methods (20). Briefly, 100-ml asexual blood stage cultures of *P. falciparum* NF54 were grown to 7% to 10% parasitemia following a triple synchronization with 5% (wt/vol) D-sorbitol. To induce gametocyte formation, cultures were given 50% spent media for 24 h, followed by daily fresh complete media changes thereafter. Postinduction, the medium was supplemented with 50 mM *N*-acetylglucosamine (NAG) for 9 days to prevent reinvasion of asexual stage parasites. At 48 h after induction, magnetically activated cell sorting (MACS) was performed, followed by sorbitol synchronization the next day. Cultures were followed by daily blood film to determine the quantity and maturation of the gametocytes. To perform the dose-response assay, 50 nl of test compounds (12.5 to 2.12×10^{-4} μM) was first prespotted into black clear-bottom 384-well plates (Greiner) using an acoustic transfer system (ATS) (Biosero). Stage-specific gametocyte cultures were diluted to 0.50% gametocytemia using serum-free screening media at 1.25% hematocrit, of which 40 μl was dispensed per well. NAG was added (50 mM) to screening assays containing gametocyte stages I to IV but not stage V. Breathable metal lids were used to cover the plates, which were incubated at 37°C for 72 h under low oxygen conditions. A solution of MitoTracker red CMXRos (2.5 μM) (Life Technologies) and saponin (0.13% wt/vol) (ACROS Organics; cat. no 419231000) was prepared in screening media, and 10 μl was added to each plate well postincubation. Plates were reincubated at 37°C for 90 min to allow for complete lysis. Test plates were then sealed with adhesive aluminum lids. Images were acquired using an Operetta high-content imaging system (PerkinElmer), and image analysis was handled by the onboard Harmony software. All assays were conducted in biological duplicate. Data were normalized against controls, and nonlinear regression analysis was performed in Prism 7 (GraphPad Software, La Jolla, CA) to determine IC_{50}s (log inhibitor versus normalized response – variable slope).

Dual gamete formation assay. MIPS-0004373 and Gentian violet (positive control) were plated onto 384-well plates in dose response using a Tecan D300e digital dispenser. The *P. falciparum* dual gamete formation assay was performed as described by Delves et al. (22). Briefly, gametocyte cultures of NF54 strain *P. falciparum* parasites were initiated at 1% ring parasitemia, and the culture medium was changed while maintaining parasites and medium at 37°C at all times. On day 14 after induction, when male stage V gametocytes showed high levels of exflagellation when induced, 50 μl of culture at 12.5 million cells per ml (approximately 2% to 4% gametocytemia) was dispensed into each well of compound-treated plates at 37°C. Gametocytes were incubated with compounds for 48 h before gametogenesis was induced by briefly cooling the plate at 4°C and by the addition of ookinete medium containing xanthurenic acid and a Cy3-conjugated antibody specific for Pfs25. Exflagellation was read 20 min after induction by automated brightfield microscopy, and exflagellation centers were identified using custom automated software. Afterward, the plate was maintained at 26°C in the dark to allow emerged female gametes to express the surface marker Pfs25. At 24 h later, female gametes were detected by automated fluorescence microscopy and quantified by custom automated software. Inhibition of male and female gametogenesis was calculated with reference to positive (12.5 μM Gentian violet) and negative (DMSO) controls using the following formula:

$$\%\,\text{inhibition} = 100 - \left\{\left[(\text{test compound} - \text{positive control})/(\text{negative control} - \text{positive control})\right] \times 100\right\}$$

Compounds were tested in four independent replicates.

***P. cynomolgi* liver stage assay.** For each batch of *P. cynomolgi* sporozoites required, one rhesus macaque was infected with blood stage parasites and mosquitoes were fed at the appropriate time point and monitored for infection rate (44). Sporozoites were harvested from *P. cynomolgi* -infected mosquitoes at around 16 days after the infected blood meal. *In vitro* infections of primary rhesus hepatocytes with *P. cynomolgi* sporozoites (spz) were performed according to Zeeman et al. (44). At day 6 postinfection (p.i.), the assays were fixed and stained with anti-*P. cynomolgi*-Hsp 70 rabbit antiserum and a fluorescein isothiocyanate (FITC)-labeled secondary antibody (goat anti-rabbit). Plates were analyzed with the Operetta high-content imaging system, differentially counting hypnozoites and developing EEFs, based on parasite size (44).

***P. berghei* liver stage assay.** Cell maintenance and liver stage activity were evaluated using methods described previously (23). Briefly, 3×10^3 HepG2-A16-CD81^{EGFP} cells were plated per well (5 μl) of

1,536-well, white, opaque-bottom plates (ref no. 789173-F; Greiner Bio-One) in Dulbecco's modified Eagle's medium (DMEM; Invitrogen, Carlsbad, USA) (supplemented with 10% fetal calf serum [FCS], 0.29 mg/ml glutamine, 100 units penicillin, and 100 μg/ml streptomycin). Cells were allowed to adhere for 2 to 4 h before test compounds were added (50 nl/well) in dose-response titrations (50×10^{-4} to 2.82×10^{-4} μM) using a Gen 4 acoustic transfer system (Biosero) for an 18-h preincubation. Atovaquone (1 μM) and puromycin (5 μM) were used as positive controls for infected and cytotoxicity plates, respectively. DMSO (0.5%) was used as the negative control in all plates. The next day, *P. berghei*-ANKA-GFP-Luc-SM_{CON} sporozoites were dissected from infected *Anopheles stephensi* mosquitoes, which were purchased from the insectary core at New York University. Parasite yields were quantified by phase-contrast microscopy and diluted to 200 sporozoites/μl in media (supplemented with 5$\times$ penicillin and streptomycin to inhibit contamination from mosquito debris). A total of 5 μl of this solution was dispensed (final well volume, 10 μl) into each well of an infected plate from a single tip bottle valve liquid handler (GNF), followed by a 3-min centrifugation (Eppendorf 5810 R) at 330 $\times$ *g* and with low brake. The addition of hepatocytes and compounds was identical for plates evaluating cytotoxicity (uninfected), with a final 5 μl of clean media added to each well (final well volume, 10 μl). All plates were incubated at 37°C (5% CO_2) and high relative humidity to mitigate media evaporation from wells.

After 48 h of incubation, infected plates were inverted and spun at 150 $\times$ *g* for 30 s to remove media. BrightGlo (Promega) was then added (2 μl) to each well using a MicroFlo liquid handler (BioTek). Immediately after the addition, plates were tapped gently to ensure the reagents made contact with the cells before bioluminescence was read using an EnVision multilabel plate reader (PerkinElmer). CellTiter-Glo (Promega) was first diluted 1:1 before it could be used to quantify bioluminescence in the cytotoxicity assay. Uninfected plates were inverted and spun as before, prior to dispensing 2 μl of diluted CellTiter-Glo in each plate well. Plates were tapped gently and left for 10 min before reading with an EnVision multilabel plate reader.

For both infected and uninfected assays, IC_{50}s were calculated by normalizing data to controls before fitting a nonlinear regression model (log inhibitor versus normalized response – variable slope) using Prism 7 (GraphPad Software, La Jolla, CA).

***In vivo* efficacy of MIPS-0004373 in the modified Thompson test.** Animal Resources Centre (ARC; Perth, Western Australia) female mice (aged 5 to 7 weeks old, mean body mass of 28.4 $\pm$ 0.9 g) in groups of six were infected with 2×10^6 *P. berghei* ANKA strain-infected RBCs on day 0 (D0). By day 3 (D + 3) p.i., parasitemia was typically about 1% to 3%. The MIPS-0004373-treated groups were administered 2-fold increases in the MIPS-0004373 dose (e.g., 2 to 64 mg/kg/day). The reference drugs artesunate and chloroquine were used to gain an insight into the performance of the modified Thompson test at an oral dose of 64 mg/kg/day. MIPS-0004373 and artesunate were prepared in Milli-Q water containing 10% ethanol and 10% Tween 80. Chloroquine was dissolved in Milli-Q water. The drugs were administered via oral gavage on days D + 3, D + 4, and D + 5 postinfection at 24-h intervals. Blood samples for flow cytometry and thin blood films were taken daily for 9 to 10 days and then twice weekly thereafter until the end of the test on day +31.

The degree of infection (i.e., parasitemia) was determined by flow cytometry (FC500; Beckman Coulter) using acridine orange as the nucleic acid stain as described by Hein-Kristensen et al. (45) with quality assurance using microscopy. The blood samples for flow cytometry and preparation of thin blood films were collected by clipping the mouse's tail tip with a scalpel blade and milking a drop of blood (about 20 μl). The thin blood film slides were stained with Giemsa for microscopy analysis. For the assessment of radical cure in the modified Thompson test, recurrence of *P. berghei* infection was tabulated for 31 days, at which time all mice surviving that were blood film negative were deemed cured.

Ethical approval. All rhesus macaques (*Macaca mulatta*) used in this study were captive bred for research purposes and were housed at the Biomedical Primate Research Centre (BPRC) facilities under compliance with the Dutch law on animal experiments, European directive 2010/63/EU, and with the "Standard for humane care and use of Laboratory Animals by Foreign institutions" identification no. A5539-01, provided by the Department of Health and Human Services of the USA National Institutes of Health (NIH). The BPRC is an AAALAC-certified institute. Prior to the start of monkey experiments, protocols were approved by the local independent ethical committee, according to Dutch law. The procedures used for the *in vivo* efficacy studies in mice were in accordance with the Australian Code of Practice for the Care and Use of Animals for Scientific Purposes. The ethical approval to conduct the tolerability and efficacy study of MIPS-0004373 in the *P. berghei*-mouse model using the modified Thompson test was approved by the Defense Animal Ethics Committee, Australian Defense Organisation (approval no. 3/2014, 03/2015, and 02/2016).

Data availability. Raw sequencing data were deposited to the NCBI Sequence Read Archive under accession no. PRJNA748017.

SUPPLEMENTAL MATERIAL

Supplemental material is available online only.

SUPPLEMENTAL FILE 1, PDF file, 1.7 MB.

SUPPLEMENTAL FILE 2, XLSX file, 0.01 MB.

ACKNOWLEDGMENTS

We are grateful to Kerryn Rowcliffe for technical support with the *in vitro* dormancy assay and thank the Australian Red Cross Blood Service for the provision of human blood,

plasma, and sera for *in vitro* cultivation of *P. falciparum* lines at Monash University, ADFMIDI, and Griffith University. We also thank Donna MacKenzie, Geoff Birrell, Ivor Harris, and Stephen McLeod-Robertson for the *in vivo* efficacy testing of MIPS-0004373 in the *P. berghei*-rodent model. We thank Nicole van der Werff and Ivonne Nieuwenhuis for expert help with the *P. cynomolgi* drug assays.

The views expressed in this article are those of the authors and do not necessarily reflect those of the Australian Defense Force Joint Health Command or any extant Australian Defense Force policy. Funding support has been provided by the Australian National Health and Medical Research Council (NHMRC) project grant no. APP1102147 and fellowships to D.J.C. (no. APP1148700) and J.B.B. (no. APP1117602). A.-M.Z. and C.H.M.K. were supported by the Medicines for Malaria Venture (MMV). M.R.L. was supported in part by a Ruth L. Kirschstein Institutional National Research Award from the National Institute for General Medical Sciences (T32 GM008666). Gametocyte time-to-kill and AO female gamete studies were supported by an MMV grant to V.M.A. Gamete formation screening was supported by an MMV grant to J.B. (RD-08-2800) and an Investigator Award from Wellcome to J.B. (100993/Z/13/Z).

REFERENCES

1. Noor A, Aponte J, Aregawi M, Barrette A, Biondi N, Knox T, Patouillard E, Williams R. 2017. World Malaria Report 2017. WHO, Geneva, Switzerland.
2. Dondorp AM, Yeung S, White L, Nguon C, Day NPJ, Socheat D, von Seidlein L. 2010. Artemisinin resistance: current status and scenarios for containment. Nat Rev Microbiol 8:272–280. https://doi.org/10.1038/nrmicro2331.
3. Yeung S, Socheat D, Moorthy V, Mills A. 2009. Artemisinin resistance on the Thai-Cambodian border. Lancet 374:1418–1419. https://doi.org/10.1016/S0140-6736(09)61856-0.
4. Burrows JN, Duparc S, Gutteridge WE, Hooft van Huijsduijnen R, Kaszubska W, Macintyre F, Mazzuri S, Möhrle JJ, Wells TNC. 2017. New developments in anti-malarial target candidate and product profiles. Malar J 16:26. https://doi.org/10.1186/s12936-016-1675-x.
5. Burrows J, Hooft van Huijsduijnen R, Mohrle J, Oeuvray C, Wells T. 2013. Designing the next generation of medicines for malaria control and eradication. Malar J 12:187. https://doi.org/10.1186/1475-2875-12-187.
6. Ban K, Duffy S, Khakham Y, Avery VM, Hughes A, Montagnat O, Katneni K, Ryan E, Baell JB. 2010. 3-Alkylthio-1,2,4-triazine dimers with potent antimalarial activity. Bioorg Med Chem Lett 20:6024–6029. https://doi.org/10.1016/j.bmcl.2010.08.065.
7. Priebbenow DL, Mathiew M, Shi D-H, Harjani JR, Beveridge JG, Chavchich M, Edstein MD, Duffy S, Avery VM, Jacobs RT, Brand S, Shackleford DM, Wang W, Zhong L, Lee G, Tay E, Barker H, Crighton E, White KL, Charman SA, De Paoli A, Creek DJ, Baell JB. 2021. Discovery of potent and fast-acting antimalarial bis-1,2,4-triazines. J Med Chem 64:4150–4162. https://doi.org/10.1021/acs.jmedchem.1c00044.
8. Xue L, Shi DH, Harjani JR, Huang F, Beveridge JG, Dingjan T, Ban K, Diab S, Duffy S, Lucantoni L, Fletcher S, Chiu FCK, Blundell S, Ellis K, Ralph SA, Wirjanata G, Teguh S, Noviyanti R, Chavchich M, Creek D, Price RN, Marfurt J, Charman SA, Cuellar ME, Strasser JM, Dahlin JL, Walters MA, Edstein MD, Avery VM, Baell JB. 2019. 3,3′-Disubstituted 5,5′-bi(1,2,4-triazine) derivatives with potent in vitro and in vivo antimalarial activity. J Med Chem 62:2485–2498. https://doi.org/10.1021/acs.jmedchem.8b01799.
9. Yang T, Xie SC, Cao P, Giannangelo C, McCaw J, Creek DJ, Charman SA, Klonis N, Tilley L. 2016. Comparison of the exposure time dependence of the activities of synthetic ozonide antimalarials and dihydroartemisinin against K13 wild-type and mutant *Plasmodium falciparum* strains. Antimicrob Agents Chemother 60:4501–4510. https://doi.org/10.1128/AAC.00574-16.
10. Klonis N, Xie SC, McCaw JM, Crespo-Ortiz MP, Zaloumis SG, Simpson JA, Tilley L. 2013. Altered temporal response of malaria parasites determines differential sensitivity to artemisinin. Proc Natl Acad Sci U S A 110:5157–5162. https://doi.org/10.1073/pnas.1217452110.
11. Witkowski B, Khim N, Chim P, Kim S, Ke S, Kloeung N, Chy S, Duong S, Leang R, Ringwald P, Dondorp AM, Tripura R, Benoit-Vical F, Berry A, Gorgette O, Ariey F, Barale J-C, Mercereau-Puijalon O, Menard D. 2013. Reduced artemisinin susceptibility of *Plasmodium falciparum* ring stages in western Cambodia. Antimicrob Agents Chemother 57:914–923. https://doi.org/10.1128/AAC.01868-12.
12. Teuscher F, Gatton ML, Chen N, Peters J, Kyle DE, Cheng Q. 2010. Artemisinin-induced dormancy in *Plasmodium falciparum*: duration, recovery rates, and implications in treatment failure. J Infect Dis 202:1362–1368. https://doi.org/10.1086/656476.
13. Veiga MI, Ferreira PE, Schmidt BA, Ribacke U, Björkman A, Tichopad A, Gil JP. 2010. Antimalarial exposure delays *Plasmodium falciparum* intra-erythrocytic cycle and drives drug transporter genes expression. PLoS One 5:e12408. https://doi.org/10.1371/journal.pone.0012408.
14. Peatey CL, Chavchich M, Chen N, Gresty KJ, Gray KA, Gatton ML, Waters NC, Cheng Q. 2015. Mitochondrial membrane potential in a small subset of artemisinin-induced dormant *Plasmodium falciparum* parasites *in vitro*. J Infect Dis 212:426–434. https://doi.org/10.1093/infdis/jiv048.
15. Tucker MS, Mutka T, Sparks K, Patel J, Kyle DE. 2012. Phenotypic and genotypic analysis of in vitro-selected artemisinin-resistant progeny of *Plasmodium falciparum*. Antimicrob Agents Chemother 56:302–314. https://doi.org/10.1128/AAC.05540-11.
16. Corey VC, Lukens AK, Istvan ES, Lee MCS, Franco V, Magistrado P, Coburn-Flynn O, Sakata-Kato T, Fuchs O, Gnädig NF, Goldgof G, Linares M, Gomez-Lorenzo MG, De Cózar C, Lafuente-Monasterio MJ, Prats S, Meister S, Tanaseichuk O, Wree M, Zhou Y, Willis PA, Gamo F-J, Goldberg DE, Fidock DA, Wirth DF, Winzeler EA. 2016. A broad analysis of resistance development in the malaria parasite. Nat Commun 7:11901. https://doi.org/10.1038/ncomms11901.
17. Lucantoni L, Duffy S, Adjalley SH, Fidock DA, Avery VM. 2013. Identification of MMV malaria box inhibitors of *Plasmodium falciparum* early-stage gametocytes, using a luciferase-based high-throughput assay. Antimicrob Agents Chemother 57:6050–6062. https://doi.org/10.1128/AAC.00870-13.
18. Lucantoni L, Fidock DA, Avery VM. 2016. A luciferase-based, high-throughput assay for screening and profiling transmission-blocking compounds against *Plasmodium falciparum* gametocytes. Antimicrob Agents Chemother 60:2097–2107. https://doi.org/10.1128/AAC.01949-15.
19. Lucantoni L, Silvestrini F, Signore M, Siciliano G, Eldering M, Dechering KJ, Avery VM, Alano P. 2015. A simple and predictive phenotypic High Content Imaging assay for *Plasmodium falciparum* mature gametocytes to identify malaria transmission blocking compounds. Sci Rep 5:16414. https://doi.org/10.1038/srep16414.
20. Plouffe DM, Wree M, Du AY, Meister S, Li F, Patra K, Lubar A, Okitsu SL, Flannery EL, Kato N, Tanaseichuk O, Comer E, Zhou B, Kuhen K, Zhou Y, Leroy D, Schreiber SL, Scherer CA, Vinetz J, Winzeler EA. 2016. High-throughput assay and discovery of small molecules that interrupt malaria transmission. Cell Host Microbe 19:114–126. https://doi.org/10.1016/j.chom.2015.12.001.
21. Ruecker A, Mathias DK, Straschil U, Churcher TS, Dinglasan RR, Leroy D, Sinden RE, Delves MJ. 2014. A male and female gametocyte functional viability assay to identify biologically relevant malaria transmission-blocking drugs. Antimicrob Agents Chemother 58:7292–7302. https://doi.org/10.1128/AAC.03666-14.

22. Delves MJ, Straschil U, Ruecker A, Miguel-Blanco C, Marques S, Dufour AC, Baum J, Sinden RE. 2016. Routine *in vitro* culture of *P falciparum* gametocytes to evaluate novel transmission-blocking interventions. Nat Protoc 11:1668–1680. https://doi.org/10.1038/nprot.2016.096.
23. Swann J, Corey V, Scherer CA, Kato N, Comer E, Maetani M, Antonova-Koch Y, Reimer C, Gagaring K, Ibanez M, Plouffe D, Zeeman A-M, Kocken CHM, McNamara CW, Schreiber SL, Campo B, Winzeler EA, Meister S. 2016. High-throughput luciferase-based assay for the discovery of therapeutics that prevent malaria. ACS Infect Dis 2:281–293. https://doi.org/10.1021/acsinfecdis.5b00143.
24. Ager AL. 1984. Rodent malaria models, p 225–264. *In* Peters W, Richards WHG (ed), Antimalarial drugs I: biological background, experimental methods, and drug resistance. Springer Berlin Heidelberg, Berlin, Heidelberg, Germany.
25. Saunders DL, Vanachayangkul P, Lon C, Royal Cambodian Armed Forces. 2014. Dihydroartemisinin-piperaquine failure in Cambodia. N Engl J Med 371:484–485. https://doi.org/10.1056/NEJMc1403007.
26. Thanh NV, Thuy-Nhien N, Tuyen NTK, Tong NT, Nha-Ca NT, Dong LT, Quang HH, Farrar J, Thwaites G, White NJ, Wolbers M, Hien TT. 2017. Rapid decline in the susceptibility of *Plasmodium falciparum* to dihydroartemisinin-piperaquine in the south of Vietnam. Malar J 16:27. https://doi.org/10.1186/s12936-017-1680-8.
27. Sanz L, Crespo B, De-Cozar C, Ding X, Llergo J, Burrows J, Garcia-Bustos J, Gamo F. 2012. *P falciparum in vitro* killing rates allow to discriminate between different antimalarial mode-of-action. PLoS One 7:e30949. https://doi.org/10.1371/journal.pone.0030949.
28. Gural N, Mancio-Silva L, Miller AB, Galstian A, Butty VL, Levine SS, Patrapuvich R, Desai SP, Mikolajczak SA, Kappe SHI, Fleming HE, March S, Sattabongkot J, Bhatia SN. 2018. *In* vitro culture, drug sensitivity, and transcriptome of *Plasmodium vivax* hypnozoites. Cell Host Microbe 23:395–406.e4. https://doi.org/10.1016/j.chom.2018.01.002.
29. Trager W, Jensen JB. 1976. Human malaria parasites in continuous culture. Science 193:673–675. https://doi.org/10.1126/science.781840.
30. Lambros C, Vanderberg JP. 1979. Synchronization of *Plasmodium falciparum* erythrocytic stages in culture. J Parasitol 65:418–420. https://doi.org/10.2307/3280287.
31. Straimer J, Gnädig NF, Witkowski B, Amaratunga C, Duru V, Ramadani AP, Dacheux M, Khim N, Zhang L, Lam S, Gregory PD, Urnov FD, Mercereau-Puijalon O, Benoit-Vical F, Fairhurst RM, Ménard D, Fidock DA. 2015. K13-propeller mutations confer artemisinin resistance in *Plasmodium falciparum* clinical isolates. Science 347:428–431. https://doi.org/10.1126/science.1260867.
32. Smilkstein M, Sriwilaijaroen N, Kelly JX, Wilairat P, Riscoe M. 2004. Simple and inexpensive fluorescence-based technique for high-throughput antimalarial drug screening. Antimicrob Agents Chemother 48:1803–1806. https://doi.org/10.1128/AAC.48.5.1803-1806.2004.
33. Johnson JD, Dennull RA, Gerena L, Lopez-Sanchez M, Roncal NE, Waters NC. 2007. Assessment and continued validation of the malaria SYBR Green I-based fluorescence assay for use in malaria drug screening. Antimicrob Agents Chemother 51:1926–1933. https://doi.org/10.1128/AAC.01607-06.
34. Boyle MJ, Wilson DW, Richards JS, Riglar DT, Tetteh KK, Conway DJ, Ralph SA, Baum J, Beeson JG. 2010. Isolation of viable *Plasmodium falciparum* merozoites to define erythrocyte invasion events and advance vaccine and drug development. Proc Natl Acad SciDefine Erythrocyte Invasion Events and Advance Vaccine and Drug Development. Proc Natl Acad Sci U S A 107:14378–14383. https://doi.org/10.1073/pnas.1009198107.
35. Witkowski B, Amaratunga C, Khim N, Sreng S, Chim P, Kim S, Lim P, Mao S, Sopha C, Sam B, Anderson JM, Duong S, Chuor CM, Taylor WRJ, Suon S, Mercereau-Puijalon O, Fairhurst RM, Menard D. 2013. Novel phenotypic assays for the detection of artemisinin-resistant *Plasmodium falciparum* malaria in Cambodia: *in-vitro* and *ex-vivo* drug-response studies. Lancet Infect Dis 13:1043–1049. https://doi.org/10.1016/S1473-3099(13)70252-4.
36. Izumo A, Tanabe K, Kato M. 1987. A method for monitoring the viability of malaria parasites (*Plasmodium yoelii*) freed from the host erythrocytes. Trans R Soc Trop Med Hyg 81:264–267. https://doi.org/10.1016/0035-9203(87)90235-5.
37. Plouffe D, Brinker A, McNamara C, Henson K, Kato N, Kuhen K, Nagle A, Adrián F, Matzen JT, Anderson P, Nam T-G, Gray NS, Chatterjee A, Janes J, Yan SF, Trager R, Caldwell JS, Schultz PG, Zhou Y, Winzeler EA. 2008. *In silico* activity profiling reveals the mechanism of action of antimalarials discovered in a high-throughput screen. Proc Natl Acad Sci U S A 105:9059–9064. https://doi.org/10.1073/pnas.0802982105.
38. Cowell AN, Istvan ES, Lukens AK, Gomez-Lorenzo MG, Vanaerschot M, Sakata-Kato T, Flannery EL, Magistrado P, Owen E, Abraham M, LaMonte G, Painter HJ, Williams RM, Franco V, Linares M, Arriaga I, Bopp S, Corey VC, Gnädig NF, Coburn-Flynn O, Reimer C, Gupta P, Murithi JM, Moura PA, Fuchs O, Sasaki E, Kim SW, Teng CH, Wang LT, Akidil A, Adjalley S, Willis PA, Siegel D, Tanaseichuk O, Zhong Y, Zhou Y, Llinás M, Ottilie S, Gamo FJ, Lee MCS, Goldberg DE, Fidock DA, Wirth DF, Winzeler EA. 2018. Mapping the malaria parasite druggable genome by using *in vitro* evolution and chemogenomics. Science 359:191–199. https://doi.org/10.1126/science.aan4472.
39. McKenna A, Hanna M, Banks E, Sivachenko A, Cibulskis K, Kernytsky A, Garimella K, Altshuler D, Gabriel S, Daly M, DePristo MA. 2010. The Genome Analysis Toolkit: a MapReduce framework for analyzing next-generation DNA sequencing data. Genome Res 20:1297–1303. https://doi.org/10.1101/gr.107524.110.
40. Van der Auwera GA, Carneiro MO, Hartl C, Poplin R, Del Angel G, Levy-Moonshine A, Jordan T, Shakir K, Roazen D, Thibault J, Banks E, Garimella KV, Altshuler D, Gabriel S, DePristo MA. 2013. From FastQ data to high confidence variant calls: the Genome Analysis Toolkit best practices pipeline. Curr Protoc Bioinform 43:11.10.1–11.10.33. https://doi.org/10.1002/0471250953.bi1110s43.
41. Cingolani P, Platts A, Wang Le L, Coon M, Nguyen T, Wang L, Land SJ, Lu X, Ruden DM. 2012. A program for annotating and predicting the effects of single nucleotide polymorphisms, SnpEff: SNPs in the genome of *Drosophila melanogaster* strain w1118; iso-2; iso-3. Fly (Austin) 6:80–92. https://doi.org/10.4161/fly.19695.
42. Duffy S, Loganathan S, Holleran JP, Avery VM. 2016. Large-scale production of *Plasmodium falciparum* gametocytes for malaria drug discovery. Nat Protoc 11:976–992. https://doi.org/10.1038/nprot.2016.056.
43. Duffy S, Avery VM. 2013. Identification of inhibitors of *Plasmodium falciparum* gametocyte development. Malar J 12:408. https://doi.org/10.1186/1475-2875-12-408.
44. Zeeman A-M, van Amsterdam SM, McNamara CW, Voorberg-van der Wel A, Klooster EJ, van den Berg A, Remarque EJ, Plouffe DM, van Gemert G-J, Luty A, Sauerwein R, Gagaring K, Borboa R, Chen Z, Kuhen K, Glynne RJ, Chatterjee AK, Nagle A, Roland J, Winzeler EA, Leroy D, Campo B, Diagana TT, Yeung BKS, Thomas AW, Kocken CHM. 2014. KAI407, a potent non-8-aminoquinoline compound that kills *Plasmodium cynomolgi* early dormant liver stage parasites *in vitro*. Antimicrob Agents Chemother 58:1586–1595. https://doi.org/10.1128/AAC.01927-13.
45. Hein-Kristensen L, Wiese L, Kurtzhals JA, Staalsoe T. 2009. In-depth validation of acridine orange staining for flow cytometric parasite and reticulocyte enumeration in an experimental model using *Plasmodium berghei*. Exp Parasitol 123:152–157. https://doi.org/10.1016/j.exppara.2009.06.010.